Geophys J. R. astr. Soc. (1972), **31**, 111–130.

Use of LP Surface Waves for Source Characterization

Yi-Ben Tsai

(Received 1972 May 22)

Summary

The complex cepstrum technique is found to provide an effective means for removing undesirable modulations of surface wave spectra caused by interference of either multiple sources or multipath propagation. This technique has greatly enhanced the utility of surface wave spectra for characterization of seismic sources. An empirical analysis of surface wave spectra on a regional basis is made on seismic events in the Arctic Ocean and the Eurasian Continent. The results indicate that: (1) the spectral shapes of Rayleigh waves often are similar among events in the same epicentral area but vary substantially from one epicentral area to another, (2) a great majority of earthquakes can be differentiated from underground nuclear explosions based on spectral shapes of Rayleigh waves, and (3) spectral shapes of Love waves do not vary as much as Rayleigh waves from one epicentral area to another. Finally, a method for systematically finding the source mechanism and focal depth of an earthquake using the observed and theoretical surface wave spectra are devised and tested. The results from tests of the method on several earthquakes are consistent with other independent evidence.

1. Introduction

A study to systematically utilize the amplitude spectra of surface waves for discrimination purposes has been in progress for some time. Preliminary results of this study are reported in this paper.

The observed surface wave spectra often are contaminated by erratic modulations caused by interference of secondary waves due to multipath propagation. This phenomenon is not related to the nature of seismic sources and therefore has to be removed from the observed spectra before these spectra can be used to extract information about seismic sources. It is found that the complex cepstrum technique provides an effective means for removing the undesirable spectral modulations caused by multipath interference. A brief description of the technique and two examples of applying the technique on actual surface waveforms are given in Section 2.

The structure of the crust and upper mantle as well as the characteristics of seismic sources may vary significantly from region to region. It is felt that utility of surface wave spectra for discrimination purposes will be enhanced if analysis of these spectra is made on a regional basis. Also, from the standpoint of discrimination the seismic events of medium to small magnitudes are at least as important as the seismic events of large magnitude. However, good-quality surface wave spectra for the small to medium seismic events are available often only at a very small number of recording

sites located not too far from the epicentres. Thus, there is a practical need for analysis of surface wave spectra on a regional basis if systematic use of these spectra for discrimination purposes is to be made. In Section 3, an empirical approach for analysis of surface wave spectra on a regional basis is applied to the seismic events in the Arctic Ocean and the Eurasian Continent.

Finally, an analytical method for deriving the source parameters of earthquakes through combined use of the observed and the theoretical spectra of both Love and Rayleigh waves is developed and tested on several earthquakes. The results are given in Section 4.

2. Application of the complex cepstrum technique for the spectral analysis of seismic surface waves

Utility of the amplitude spectra of surface waves for studying seismic sources is often hindered by spectral modulations caused by interference of multiple wave trains originated from multipath propagation or multiple sources. Such spectral modulations are not related to the characteristics of a seismic source and thus have to be removed before the spectra can be used to extract information about the source. The complex cepstrum technique is quite effective for removing this type of spectral modulations. Results from application of this technique to actual surface waveforms are described below.

The mathematical foundation of the complex cepstrum technique has been established by Schafer (Schafer 1969). Linville (1971) and his colleagues at Texas Instruments Incorporated have successfully applied the technique to study multipath Rayleigh waves. Since details of both the theoretical and the practical aspects of the technique can be found in the literatures cited above, only a brief summary of the technique is given here.

Mathematically, a modulated waveform, $x(t)$, consisting of multiple arrivals can be represented as convolution of a primary waveform $s(t)$ with a multipath operator $m(t)$, i.e.

$$x(t) = s(t)_* \, m(t).$$

Taking Fourier transform of this equation we have

$$X(\omega) = S(\omega).M(\omega).$$

Multiplication of the two complex spectra on the right side is transformed into addition by taking the logarithm of the preceding equation, namely,

$$\log X(\omega) = \log S(\omega) + \log M(\omega).$$

The imaginary part of $\log X(\omega)$ is made continuous. The linear component of this new function is taken off at this point. The resultant $\log X(\omega)$ is treated then as a complex 'time' series and its inverse Fourier transform is taken to yield a function $\hat{x}(t)$ called the complex cepstrum. Now a linear filter can be applied to $\hat{x}(t)$ before its direct Fourier transform is taken. This operation will be able to separate $\log S(\omega)$ and $\log M(\omega)$ as long as their 'frequency' contents do not overlap substantially. In the case of interfering seismic surface waves a 'short-pass' filter applied to $\hat{x}(t)$ will remove $\log M(\omega)$ from $\log X(\omega)$ and as a result provide an estimate of $\log S(\omega)$. On the contrary, a 'long-pass' filter on $\hat{x}(t)$ will give an estimate of $\log M(\omega)$. The complex Fourier spectrum of either $S(\omega)$ or $M(\omega)$ can be obtained at this point by taking the exponential of the filtered $\log X(\omega)$. One more performance of inverse Fourier transform will further provide the recovered primary waveform $x(t)$ or the multipath operator $m(t)$.

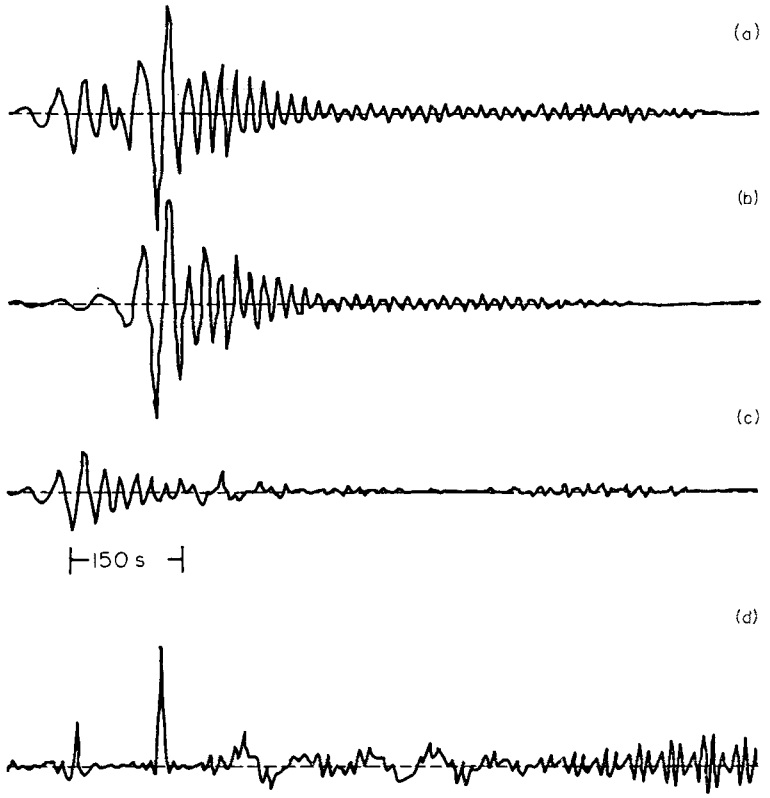

FIG. 1. Rayleigh waves from two successive earthquakes: (a) Original waveforms (b) Recovered waveform for the second earthquake; (c) Difference between (a) and (b); (d) Waveform of the multipath operator

The computer program written by Linville (1971) is adopted for use with some modifications. Two examples are given to show the effectiveness of the complex cepstrum technique for separating interfering seismic surface waves.

The first example is a composite Rayleigh waveform from two successive earthquakes located in the North Atlantic Ridge. According to PDE, the origin time and epicentre location of these two events are listed below:

	Date	Origin time	Epicentre	m_b
Event 1	70-12-22	20:51:16·2	28·3° N 43·9° W	5·3
Event 2	70-12-22	20:53:04·3	28·3° N 43·9° W	5·4

The waveform prior to application of the complex cepstrum technique is shown by Trace A in Fig. 1. This waveform is obtained by applying a 0·02–0·05 Hz bandpass filter to the digital seismogram recorded by a high-gain long-period instrument located at Ogdensburg (OGD), New Jersey. The amplitude spectrum corresponding to this waveform is shown by the dashed curve in Fig. 2. The periodic modulation of the spectrum is caused by interference of the two successive Rayleigh wavetrains. After application of the complex cepstrum technique, the primary wavetrain due to the second but larger earthquake is largely recovered and shown by Trace B in Fig. 1. The corresponding Fourier amplitude spectrum is shown by the solid line in Fig. 2. Contrary to the original spectrum this spectrum is practically free from modulations. By subtracting Trace B from Trace A it is possible to obtain the secondary wavetrain which is due to the first but smaller earthquake. Trace C in Fig. 1 shows this wavetrain.

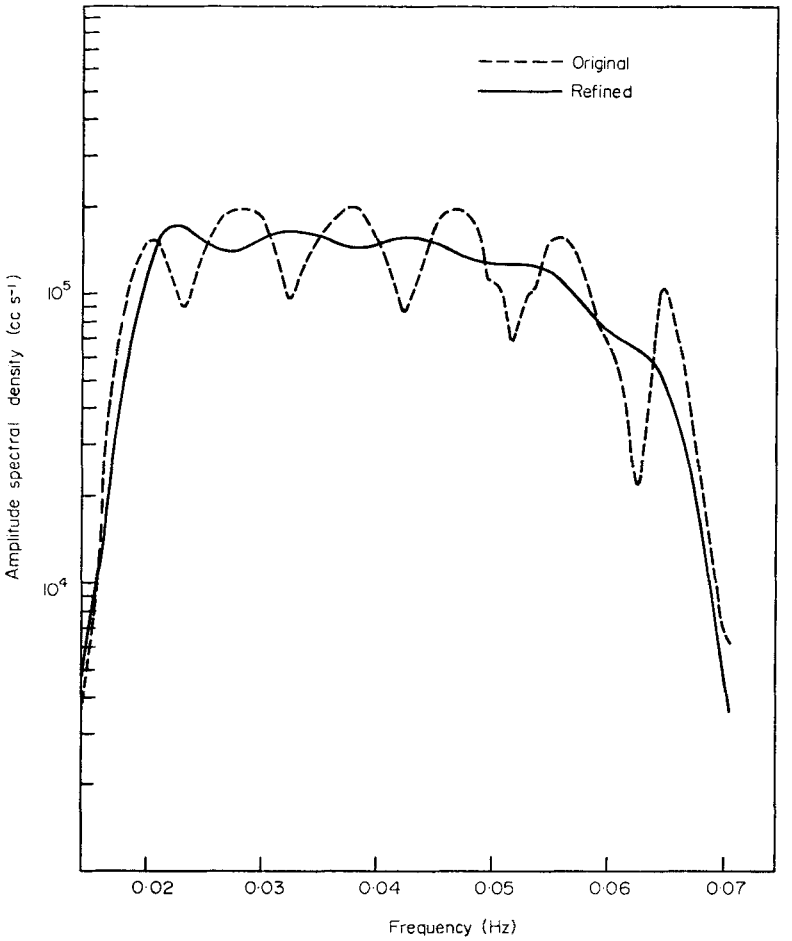

FIG. 2. Amplitude spectral density of the first two waveforms in Fig. 1, uncorrected for instrument response.

The resemblance between the primary (Trace B) and the secondary (Trace C) wavetrains is remarkable.

In addition to the primary waveform, the complex cepstrum technique can also provide the waveform of the multipath operator. For the present example this multipath operator is shown by Trace D in Fig. 1. The two impulses on this trace mark the two successive arrivals separated by 108 s. They also indicate that Rayleigh waves due to the first earthquake are about half as large as the second earthquake. It is interesting to point out that the delay time of 108 s between the two impulses as indicated by Trace D is exactly the same as the difference between the origin times of the two earthquakes, as given in PDE.

The second example is a long wavetrain of Love waves from two successive earthquakes at the same location in the Kirgiz–Sinkiang border region. According to PDE, the origin time and epicentre of these earthquakes are given below:

	Date	Origin time	Epicentre	m_b
Event 1	71-03-24	20:54:28·6	41·5° N 79·5° E	5·3
Event 2	71-03-24	21:01:54·9	41·4° N 79·4° E	5·3

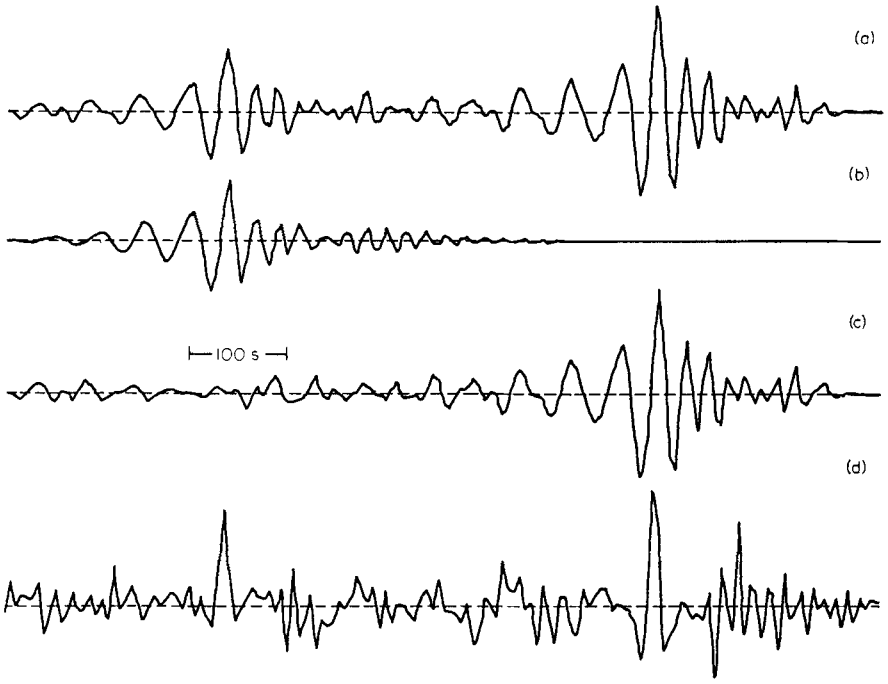

FIG. 3. Love waves from two successive earthquakes: (a) Original waveform; (b) Recovered waveform for the first earthquake; (c) Difference between (a) and (b); (d) Waveform of the multipath operator.

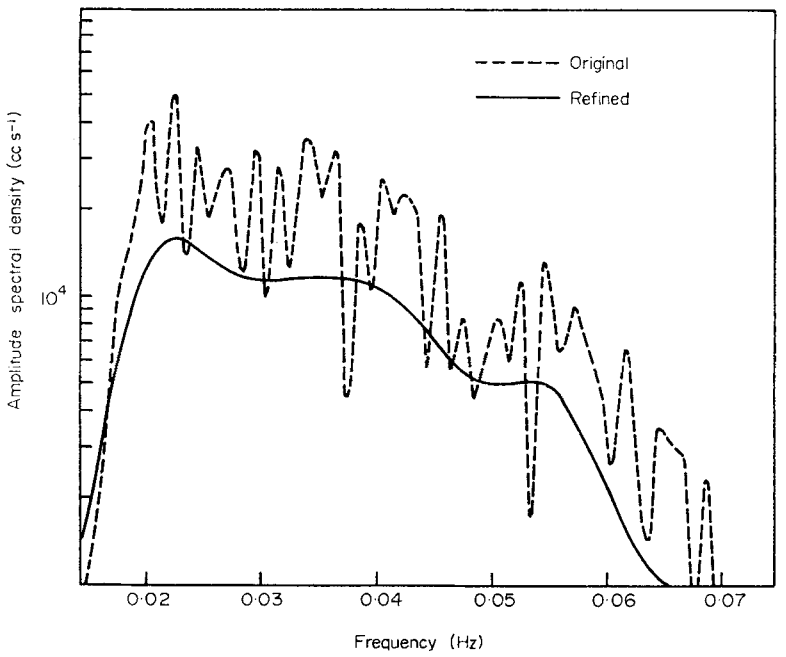

FIG. 4. Amplitude spectral density of the first two waveforms in Fig. 3, uncorrected for instrument response.

The waveform, as shown on Trace A in Fig. 3, is obtained by applying a 0·02–0·05 Hz bandpass filter to the original digital seismogram recorded by a high-gain long-period instrument located at Chiangmai (CHG), Thailand, The corresponding Fourier amplitude spectrum is shown by the dashed curve in Fig. 4. The spectrum is dominated by the rapid, regular modulation caused by interference of the two wavetrains. In addition, there exists a slower and less regular type of modulation which is due to interference of multipath propagation suffered by individual wavetrains. The existence of such modulation due to multipath propagation can be ascertained by looking at the spectrum of a single wavetrain due to either one of the two earthquakes.

Application of the complex cepstrum technique to the waveform on Trace A of Fig. 3 yields a waveform shown on Trace B of the same figure. This new waveform contains only the wavetrain due to the first earthquake. The corresponding spectrum, as given by the solid curve in Fig. 4, has been cleared of all types of modulations. This example shows that the complex cepstrum technique can remove effectively all interfering wavetrains regardless of their cause due to multiple source or multipath propagation.

The wavetrain pertaining to the second earthquake is obtained by subtracting trace B from Trace A of Fig. 3 and shown on Trace C of the same figure. The multipath operator as shown on Trace D again indicates two distinctive arrivals separated by 446 s in time. However, the waveform of this operator is far more complicated when compared with that of the previous example shown on Trace D of Fig. 1. This complication results from interference of multipath propagation which is absent in the previous example.

In summary, the complex cepstrum technique is shown to be very effective in removing spectral modulations of surface waves resulting from multiple sources or multipath propagation. The output from operation of the technique can be conveniently checked both in the time domain as well as in the frequency domain. Although we are concerned here only with the amplitude spectrum, it should be pointed out that the phase spectrum is also 'cleaned-up' in the process. Therefore, the complex cepstrum technique is potentially useful, not only for source study using the amplitude spectra of surface waves, but also for dispersion study using the phase spectra.

More examples on the application of the technique for removing the effects of multipath propagation on surface wave amplitude spectra are given in the following section.

3. Preliminary results from spectral analysis of surface waves on a regional basis

It is well known that both the characteristics of seismic source and the structure of the crust and upper mantle may vary greatly from region to region. Meanwhile, we also know that the source characteristics of earthquakes in a specific tectonic region often show common patterns. Thus, it becomes highly desirable from the standpoint of seismic discrimination to study seismic surface waves on a regional basis. Furthermore, surface waves generated by seismic events of medium to low magnitudes are recorded with good quality usually only at seismographic stations located not too far from the epicentres. Therefore, analysis of surface wave spectra on a regional basis is also a practical necessity if these spectra are to be used to extract information about the source characteristics of relatively small seismic events. Surface wave spectra analysed in this manner are potentially useful not only because they can provide diagnostic criteria of their own for seismic discrimination, but also because they may provide explanations for anomalous $M_s : m_b$ behaviour occasionally observed for some events. Love waves are no less useful than Rayleigh waves in this

regard. Thus, whenever the data are available, Love waves will be included in the analysis.

Recently, a study of surface wave spectra on a regional basis has been undertaken. Preliminary results of this study are described below.

Amplitude spectra of surface waves recorded by the high-gain long-period seismographs operated by Lamont–Doherty Geological Observatory at selected sites are obtained for 28 seismic events located in the Arctic Ocean and the Eurasian Continent ranging from Turkey in the west to Yunnan Province, China, in the east. Detailed information on the epicentre, origin time, and magnitude of these events is taken from PDE and listed in Table 1. A map showing the locations of the epicentres and two of the four recording sites, CHG and EIL, is given in Fig. 5. Two of the 28 events are presumed to be underground nuclear explosions in Novaya Zemlya. The remaining 26 events are earthquakes with magnitude m_b ranging from 4·5 to 5·4, with one exception of $m_b = 6·0$. Taking into account the instrument response, the discussion will be made based on the spectra over the frequency band of 0·02–0·05 Hz. Since in this frequency band the change of spectral shape due to attenuation is insignificant (Tsai & Aki 1971), no attempt is made to correct for the effects of attenuation on the spectra. Furthermore, the correction for magnification as a function of frequency will not be made at this point. Thus, all the spectra presented in this section bear the same numerical unit as the original digital records. The spectra of surface waves from these seismic events are compared below according to their epicentral locations.

Table 1

The origin time, epicentre, and magnitude of the seismic events studied

No.	Date	Time	Latitude	Longitude	Depth	m_b	Sites
A1	1971.10.14	05:59:57·1	73·3° N	55·1° E	0	6·7	FBK
A2	1971.09.27	05:59:55·0	73·4° N	55·1° E	0	6·4	OGD
A3	1971.08.22	11:07:21·0	83·0° N	6·5° W	N	4·6	OGD
A4	1971.01.27	20:45:42·8	76·7° N	7·0° E	31	4·9	FBK, OGD
A5	1971.01.29	08:33:49·7	78·8° N	8·0° E	N	4·8	FBK, OGD
A6	1971.01.28	11:03:49·5	76·5° N	8·1° E	N	4·5	FBK, OGD
A7	1971.01.31	04:33:27·4	76·6° N	7·3° E	N	4·7	FBK, OGD
A8	1971.01.26	08:08:44·1	77·1° N	8·5° E	N	4·6	FBK, OGD
A9	1971.06.04	09:10:02·7	84·6° N	108·0° E	N	5·1	OGD
A10	1971.08.21	19:34:23·2	81·9° N	118·9° E	N	4·6	OGD
A11	1971.06.04	07:56:54·8	84·5° N	107·5° E	N	5·0	OGD
B1	1971.01.26	22:48:31·1	43·8° N	39·2° E	28	4·8	EIL
B2	1971.04.17	16:37:38·4	41·0° N	37·0° E	N	4·8	EIL
B3	1971.05.24	02:20:13·9	38·8° N	40·5° E	N	4·7	EIL
C1	1971.06.08	16:59:24·8	37·5° N	29·8° E	10	4·7	EIL
C2	1971.06.04	15:06:12·1	37·6° N	29·8° E	27	4·6	EIL
C3	1971.05.23	20:11:21·6	37·6° N	29·9° E	33	4·7	EIL
D1	1971.04.06	06:49:52·9	29·8° N	51·9° E	10	5·2	EIL
D2	1971.03.31	21:50:10·3	34·6° N	50·3° E	31	4·4	EIL
D3	1971.05.22	14:02:07·5	35·6° N	58·3° E	36	4·8	EIL
D4	1971.01.28	15:51:06·6	35·0° N	47·0° E	43	4·6	EIL
E1	1971.05.27	00:30:27·7	38·3° N	69·0° E	36	4·8	EIL
E2	1971.04.04	01:35:23·3	38·4° N	73·3° E	33	4·8	EIL, CHG
E3	1971.03.23	20:47:17·4	41·5° N	79·3° E	33	6·0	CHG
E4	1971.03.24	21:01:54·9	41·4° N	79·4° E	25	5·3	CHG
E5	1971.05.03	00:33:22·5	30·8° N	84·5° E	16	5·4	CHG
E6	1971.06.04	14:10:46·0	32·2° N	95·2° E	N	5·0	CHG
E7	1971.02.05	09:10:35·7	25·2° N	99·4° E	N	5·3	CHG

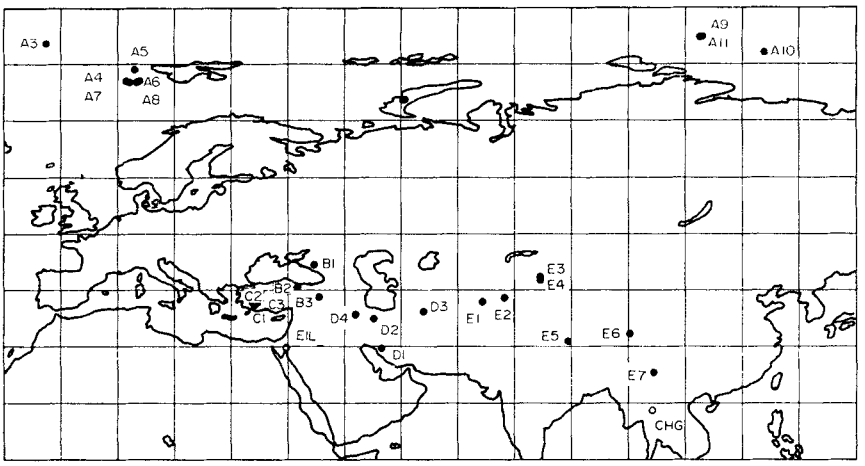

FIG. 5. Locations of the earthquakes studied and two of the LPE recording sites, CHG and EIL.

(a) *Earthquakes and explosions in the Arctic Ocean*

Fig. 6 shows Rayleigh wave spectra for two presumed underground nuclear explosions in Novaya Zemlya (Events A1 and A2), six earthquakes (Events A3–A8) in the Nansen fracture zone near Svalbard, and three other earthquakes (Events A9–A11) in the Arctic mid-oceanic ridge near Severnaya Zemlya. The spectra on the left side of the figure are from FBK (Fairbanks, Alaska) while those on the right side came from OGD (Ogdensburg, New Jersey). The instrument response for the frequency band of 0·02–0·05 Hz is essentially the same for these two sites except that magnification at OGD is slightly higher. With regard to these spectra the following remarks are appropriate.

(1) Rayleigh waves generated by the two presumed underground nuclear explosions in Novaya Zemlya as recorded at FBK for Event A1 and at OGD for Event A2 have very similar spectral content even though they are recorded at different azimuths. Both spectra increase steadily by a factor of about 10 from 0·02 to 0·04 Hz. In addition, the absolute spectral levels for the two events are also consistent with their m_b values. These observations suggest that the spectral content of Rayleigh waves from underground nuclear explosions in Novaya Zemlya do not vary significantly from event to event and with azimuth.

(2) The spectra of Rayleigh waves from the earthquakes near Svalbard have similar shapes at FBK and OGD for any given event even though the azimuths to these sites differ by about 64°. On the other hand, the shapes of spectra may change notably from event to event even though their epicentres are not too far apart. For examples, the spectra of Events A4 and A5 are different from each other at both sites in that the spectra of Event 4 decrease from 0·03 to 0·05 Hz while those of Event 5 remain virtually constant in the same frequency band. The spectra at OGD have levels about three times as high as FBK for all the five events for which Rayleigh wave spectra are available simultaneously at both sides. This factor of three difference in the spectral levels between OGD and FBK is consistent with a source mechanism of the strike-slip fault having its strike oriented in the same general direction as the Nansen fracture zone, namely in the NNW–SSE direction. Thus, the five earthquakes discussed here probably have similar transform fault source mechanisms. This type of source mechanisms has been observed by Sykes (1967) for earthquakes in many other fracture zones over the world. As for the changes in spectral shapes from one event to the other these may be attributed to the difference in focal depth.

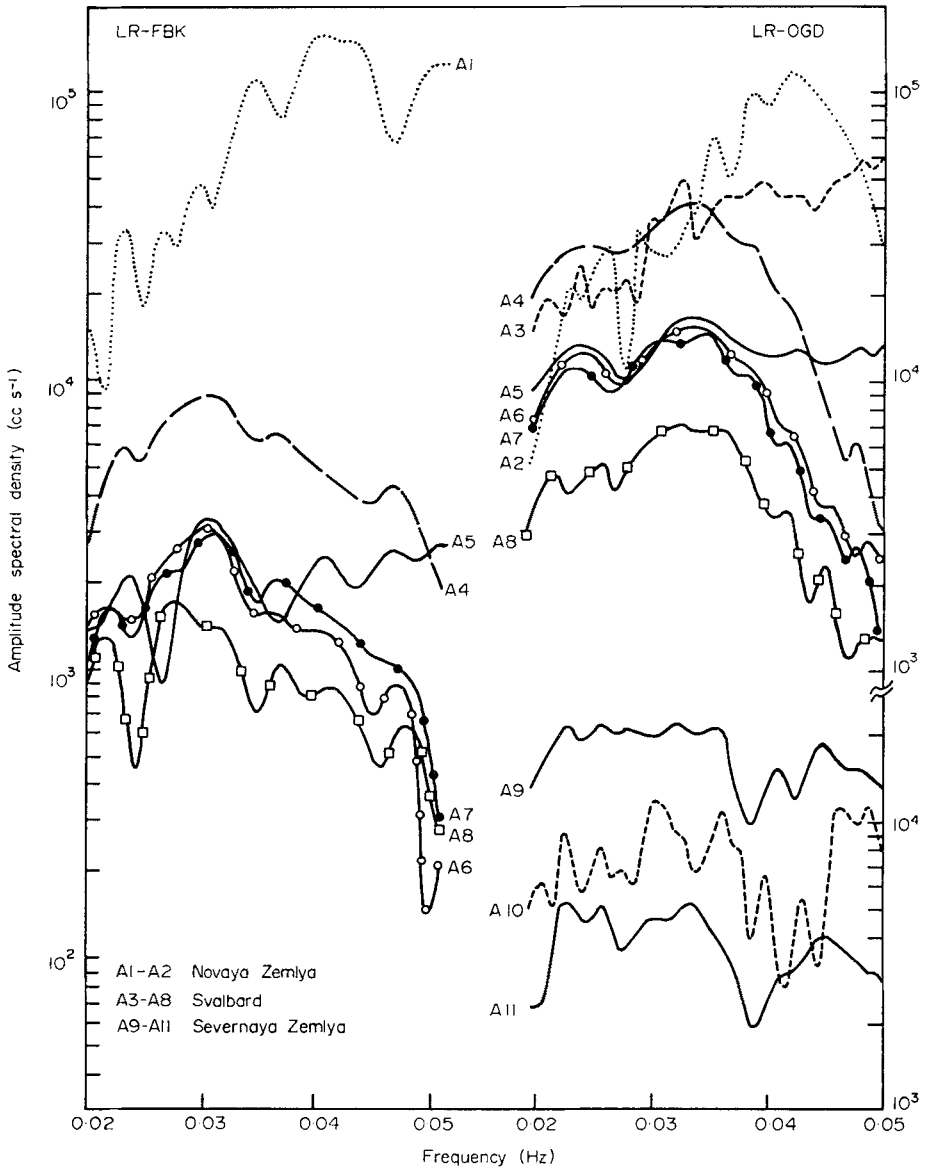

FIG. 6. Amplitude spectral density of Rayleigh waves recorded at FBK (left) and OGD (right).

(3) The general shapes of Rayleigh wave spectra from the three earthquakes near Severnaya Zemlya (Events A9, A10 and A11) as observed at OGD are very similar to each other. This implies that their focal depths and source mechanisms probably are the same. Unfortunately, the data are limited and consist of only one Rayleigh wave component at one site for each of these events. Thus, it is not possible to infer their source mechanisms.

(4) Rayleigh waves from the presumed underground nuclear explosions in Novaya Zemlya differ substantially from eight of the nine earthquakes in the Arctic Ocean analysed here. The explosions generate much greater amplitudes of Rayleigh waves in the frequency band 0·035–0·05 Hz with respect to the band 0·02–0·035 Hz

than earthquakes. The ninth earthquake in Svalbard region (Event A3) generated Rayleigh waves having a spectral content similar to underground nuclear explosions. Tsai & Aki (1971) have pointed out that a great many earthquakes can be differentiated from underground nuclear explosions using the spectra of Rayleigh waves. There still exists a small number of earthquakes which cannot be identified by this criterion. This theoretical prediction appears to be supported by these observations. It should be pointed out that there is only one single observation of Rayleigh wave spectra for this particular earthquake. It may have been possible to identify this event using surface wave spectra if data of Love waves and/or of Rayleigh waves at other sites had been available. It is interesting to note that Event A3 still can be differentiated from underground nuclear explosions using M_s:m_b criterion.

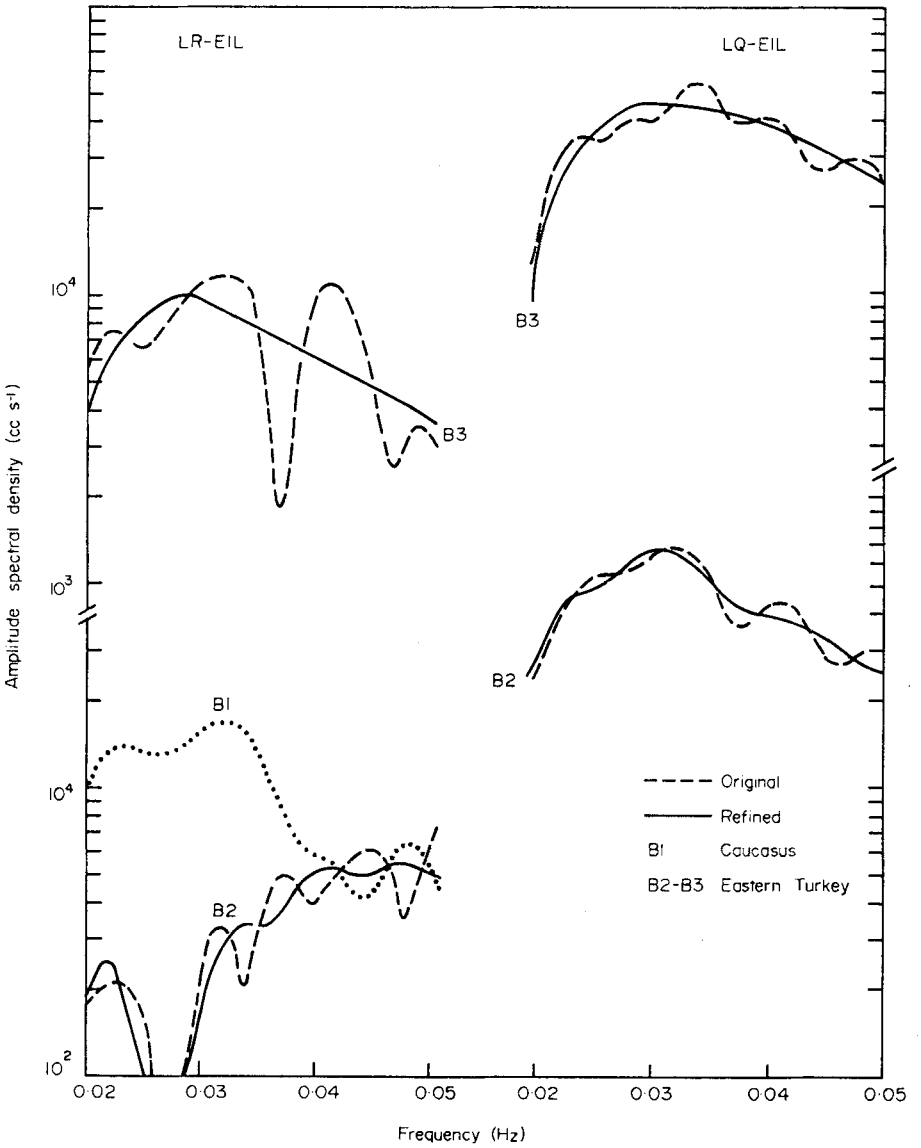

FIG. 7. Amplitude spectral density of Rayleigh (LR) and Love (LQ) waves recorded at EIL.

(b) *Earthquakes in Caucasus and Eastern Turkey*

Fig. 7 shows the spectrum of Rayleigh waves from an earthquake in Western Caucasus (Event B1) and the spectra of both Rayleigh and Love waves from two earthquakes in Eastern Turkey (Events B2 and B3). These spectra are obtained at EIL (Eilat, Israel). The dashed and solid curves represent the spectra of the same component before and after application of the complex cepstrum technique. The spectra of Rayleigh waves from these three earthquakes differ significantly from each other. On the other hand, the spectra of Love waves appears to be more predictable. This phenomenon is again consistent with what can be anticipated theoretically. From the original and the refined spectra of Rayleigh waves from Event B3 shown on the upper left corner of Fig. 7 one can see the effectiveness of the complex cepstrum technique for removing the erratic spectral modulations resulting from multipath propagation. On the other hand, the deep spectral node between frequencies 0·025–

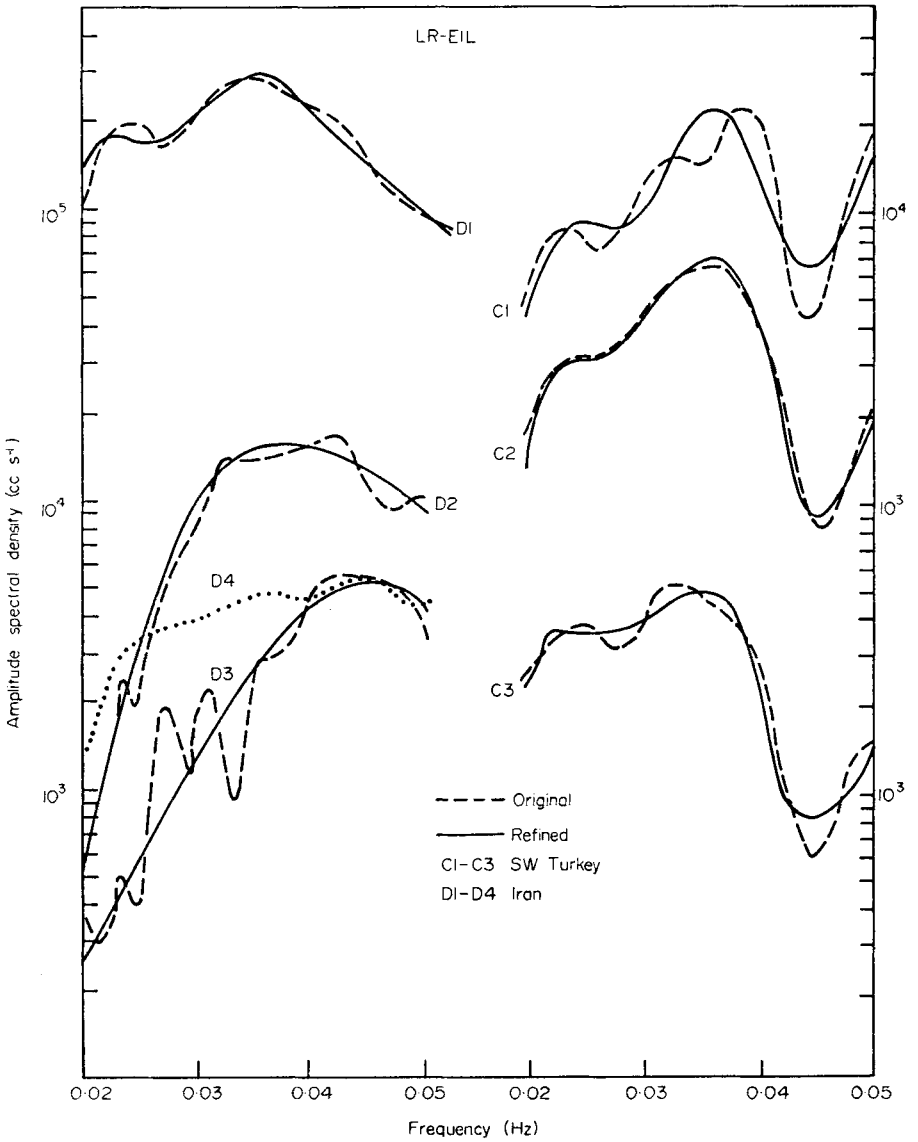

FIG. 8. Amplitude spectral density of Rayleigh waves recorded at EIL.

0·02 Hz present on the spectrum of Rayleigh waves from Event B2, as shown in the lower left corner of Fig. 7, remains unchanged by the complex cepstrum technique. This spectral node, as will be shown in a later section, is associated with focal depth rather than with multipath propagation. Thus, the result of this case is very interesting because it shows that the complex cepstrum technique is able to remove the spectral modulations due to multipath propagation without obscuring, at the same time, the spectral node related to the source mechanism and focal depth of an earthquake. In other words, the complex cepstrum technique can be used for improving the utility of seismic surface waves for extracting information about their sources. More detailed interpretation of the spectra for Events B2 and B3 will be made in the following section.

(c) *Earthquakes in south-western Turkey*

The spectra of Rayleigh waves from three earthquakes in south-western Turkey observed at EIL are shown in the right side of Fig. 8. These three events are aftershocks following an $m_b = 5{\cdot}5$ earthquake on 1971 May 12. The dashed and solid curves represent the spectra before and after application of the complex cepstrum technique. All the three spectra are practically identical in shape and marked by a deep spectral trough at about 0·045 Hz. Since the propagation path from the epicentre to the recording site EIL consists of a large segment of the eastern Mediterranean Sea that appears to be complicated and since data is available only for one component, no inference on the source parameters of these earthquakes will be made at present.

(d) *Earthquakes in Iran*

Rayleigh wave spectra of four earthquakes in Iran (Events D1–D4) observed at EIL are shown in the left side of Fig. 8. The epicentres are scattered over a large area and the shapes of Rayleigh wave spectra are varied. Since the propagation paths appear to be similar, the observed spectral differences most likely reflect the differences in source mechanism and/or focal depth. Unfortunately, the N–S component of the digital records at EIL is unusable and so corresponding Love wave spectra for most of the events discussed here are not available.

(e) *Earthquakes in Central Asia, Tibet and south-western China*

The spectra of Rayleigh and Love waves from seven earthquakes in this large area are obtained at EIL or at CHG (Chiangmai, Thailand). The spectra of Love and Rayleigh waves from Event E1, an earthquake in Tadzhik, USSR, observed at EIL are shown in the upper part of Fig. 9. The spectral level of Rayleigh waves is about three times that of Love waves at this site. Hence, EIL appears to be near the nodal direction of Love wave radiation pattern of the earthquake.

Shown in the lower part of Fig. 9 are the spectra of Love and Rayleigh waves from an earthquake (E2) located in Tadzhik–Sinkiang border region obtained at CHG. Again, the dashed and solid curves denote the spectra before and after application of the complex cepstrum technique. It can be seen from this one and the two following figures that both Love and Rayleigh waves suffer multipath propagation even though their propagation paths are entirely within the continent. Furthermore, Rayleigh waves seem to suffer a greater degree of contamination due to multipath propagation than Love waves for a given great-circle path. The effectiveness of the complex cepstrum technique for removing modulations on the spectra due to multipath interference is again convincingly demonstrated by these examples. Further interpretation of these spectra in terms of source parameters of this earthquake will be made in the following section.

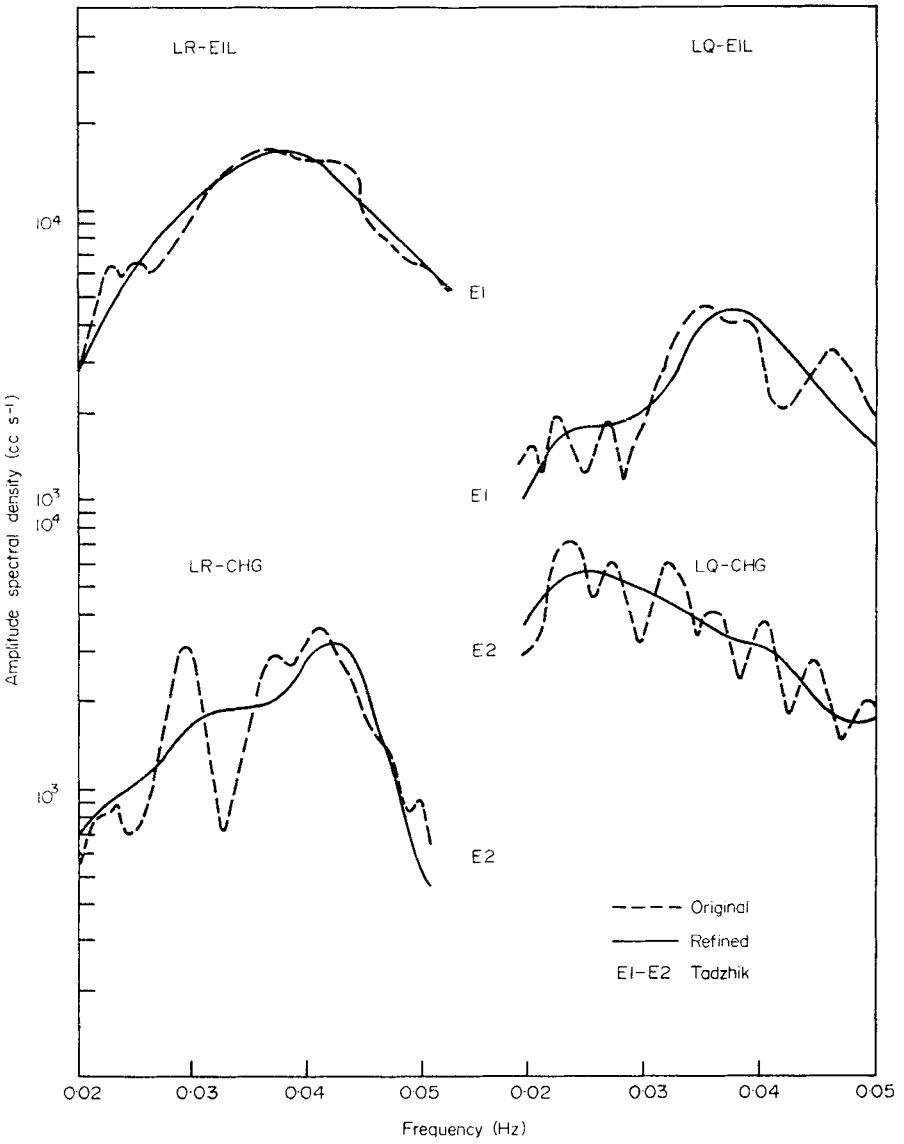

FIG. 9. Amplitude spectral density of Rayleigh (LR) and Love (LQ) waves.

Fig. 10 shows Rayleigh and Love wave spectra obtained at CHG for two earthquakes (Events E3 and E4) located at the same epicentre in Kirghiz–Sinkiang border region. The shapes of Rayleigh and Love wave spectra are nearly identical between the two earthquakes even though the spectral levels of one earthquake (Event E3) are about 20 times higher than the other (Event 4). Existence of common spectral shapes among earthquakes occurred in the same epicentral area has been observed earlier for the three earthquakes in south-western Turkey (i.e. Events C1, C2, C3). Incidentally, Event E4 is the same one earthquake which generated the second Love wave train on Trace A of Fig. 3 and which was discussed in the preceding section. The refined Love wave spectrum of Event E4 shown in Fig. 10 is remarkably similar to the one shown previously in Fig. 4. This shows that the complex cepstrum technique

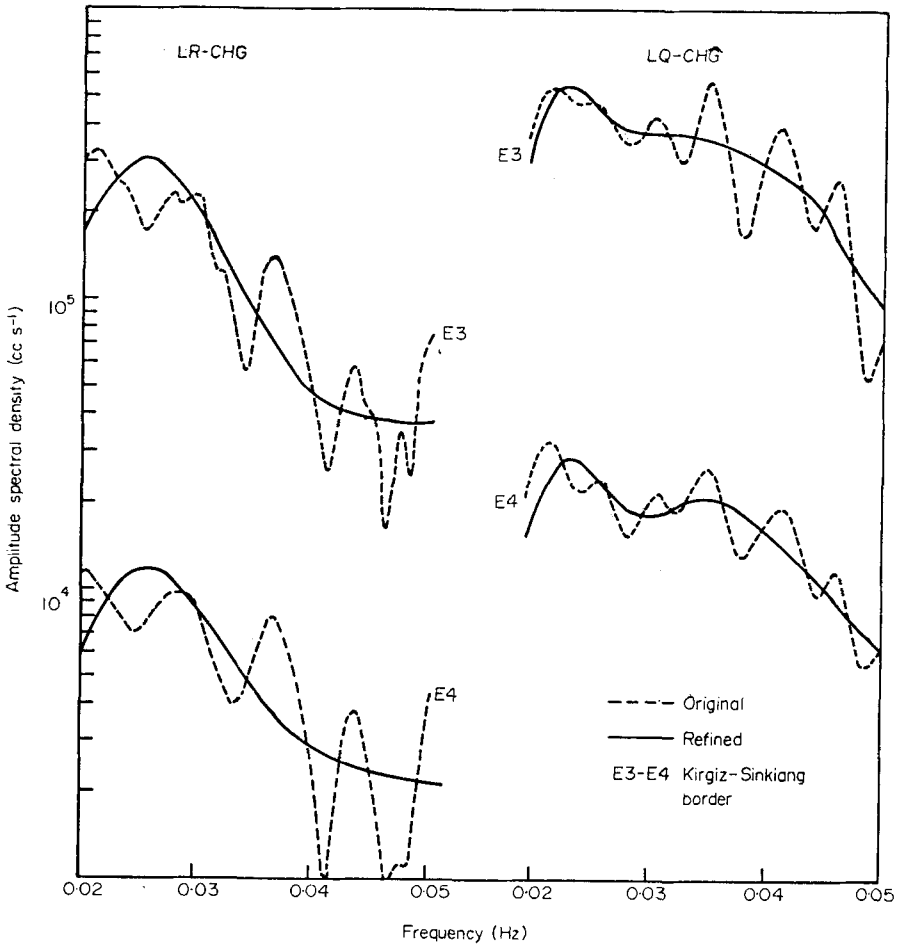

FIG. 10. Amplitude spectral density of Rayleigh (LR) and Love (LQ) waves recorded at CHG.

will have the same performance in removing the multipath interference regardless of the number of wavetrains involved.

By comparing the spectra between Event E2 on the one hand and Events E3 and E4 on the other one finds that Rayleigh waves are entirely different in their spectral shapes whereas Love waves do not vary significantly from event to event.

Fig. 11 shows Rayleigh and Love wave spectra obtained at CHG for Events E5 and E6 which are two earthquakes in Tibet. The spectrum of Rayleigh waves for a third earthquake E7 which is located in Yunnan Province, China also is given in the figure. These earthquakes are located at different epicentres, and as observed earlier, the Rayleigh wave spectral shapes differ greatly from each other. On the contrary, the Love wave spectral shapes are very much alike. In fact, the five Love wave spectra observed at CHG from Events E2 through E6 are quite similar to each other even though the earthquakes are located over a wide geographical area.

In summary, the following remarks about the spectral behaviours of surface waves from seismic events in the Arctic Ocean and the Eurasian Continent can be made.

(1) Rayleigh waves from underground nuclear explosions in Novaya Zemlya appear to have the same spectral content from event to event and varying very little

with azimuth. Furthermore, these spectra are substantially different from those of a great majority of earthquakes in the neighbouring seismic areas such as Svalbard and Severnaya Zemlya in the Arctic Ocean.

(2) The spectral shapes of both Love and Rayleigh waves from earthquakes do not change significantly from event to event for earthquakes located in the same epicentral region. This phenomenon indicates that a suite of reference spectra of surface waves may be established at a number of recording sites for seismic events in different areas. These reference spectra can be used to monitor changes in source characteristics of future seismic events taking place in these same epicentral areas.

(3) The spectral shapes of Love waves from earthquakes located in a wide area of Central Asia and Tibet do not change substantially from epicentre to epicentre. On

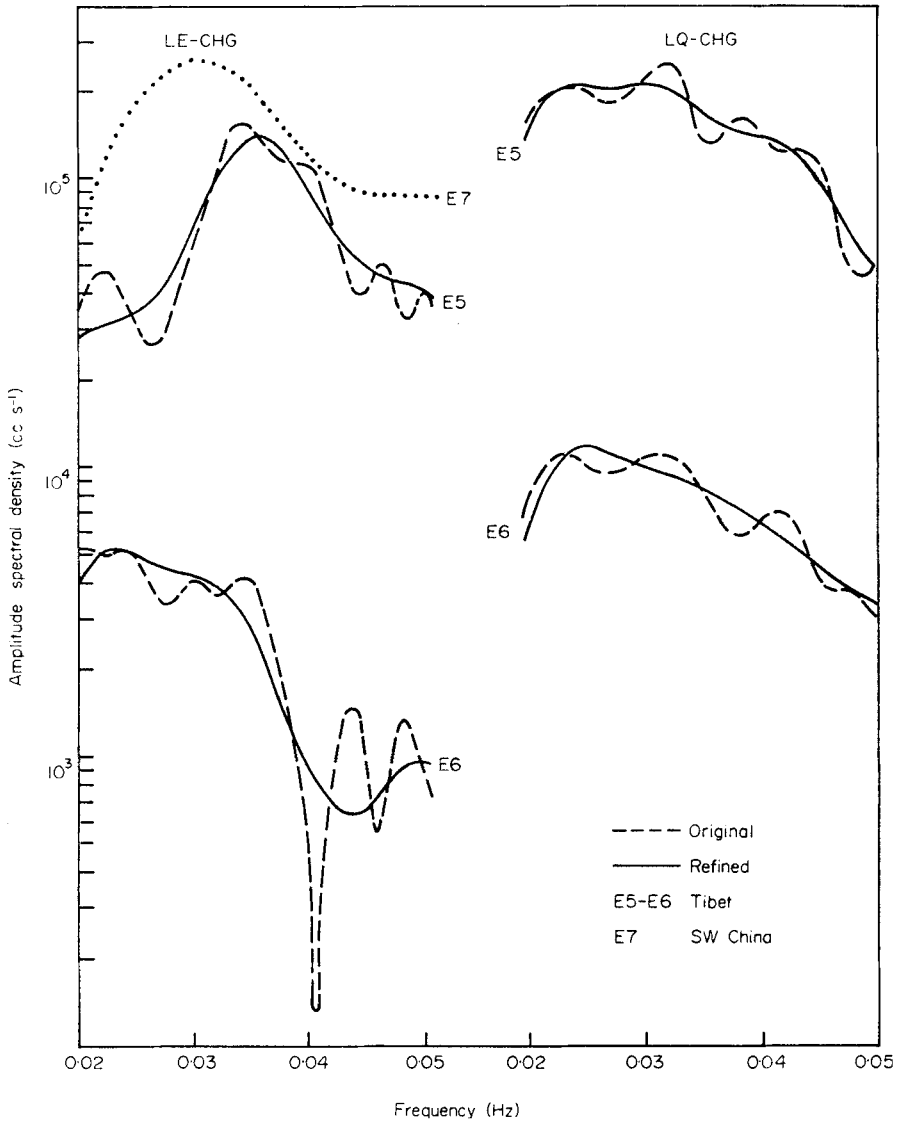

FIG. 11. Amplitude spectral density of Rayleigh (LR) and Love (LQ) waves recorded at CHG.

the contrary, the spectral shapes of Rayleigh waves from the same earthquakes differ greatly from one epicentral area to another. Although one may attribute this phenomenon to the differential effects of propagation on Rayleigh and Love waves, it is far more likely that the phenomenon resulted from differences in source mechanism and/or focal depth as predicted by theory. Thus, the large variation of Rayleigh wave spectra can be used for discrimination purposes. In the meantime, Love wave spectra may add important information on the azimuthal variation of radiation patterns.

4. Characterization of seismic sources by amplitude spectra of surface waves

This section describes an analytical method for finding the source mechanism and focal depth of an earthquake from the amplitude spectra of surface waves in a systematic fashion. For a prescribed Earth's model the theoretical spectra of Rayleigh and Love waves from a double-couple point source of a given orientation and focal depth can be computed for any azimuths by Saito's method (Saito 1967). Explicit expressions for such computations may be found in an article by Tsai & Aki (1970). For the present purpose a step function is assumed to represent the source time history. The orientation of a double couple source is specified by three parameters related to a dislocation surface, namely, the strike, the dip and slip angles of the surface. These three plus the focal depth are the four source parameters to be determined from a given set of observed spectra of Love and Rayleigh waves. The double-couple orientation determined in this way will represent the orientation of either the actual fault plane or its auxiliary plane. Such ambiguity on deciding the fault plane can only be eliminated by relying on data other than surface wave spectra, such as existing faults in the epicentral area or the distribution of aftershocks.

The amplitude spectra of surface waveforms from an earthquake recorded at a given number of sites are obtained by fast Fourier transform. If necessary, the complex cepstrum technique is applied to remove the interference of multipath propagation. These spectra are further corrected for individual instrument response and equalized to a common epicentral distance by multiplying a factor of geometrical spreading. These observed spectra are subsequently compared with theoretical spectra corresponding to a source having certain orientation and focal depth. An error count is obtained by taking the sum of squares of residuals between the observed and theoretical spectral values over all frequencies and components.

Let X_{ij}^{Q} and X_{ij}^{R} represent the observed spectra of Love and Rayleigh waves, respectively, for ith frequency and jth site. Y_{ij}^{Q} and Y_{ij}^{R} denote the corresponding theoretical spectra for a given source. An error count S is defined as the sum of squares of all residuals between the observed and theoretical spectral values, namely,

$$S = \sum_j \sum_i [(X_{ij}^{Q} - C\,Y_{ij}^{Q})^2 + (X_{ij}^{R} - C\,Y_{ij}^{R})^2]. \tag{1}$$

It can be shown that the error count S will be minimum for this particular set of Y_{ij}^{Q} and Y_{if}^{R} if

$$C = \frac{\sum_j \sum_i (X_{ij}^{Q}\,Y_{ij}^{Q} + X_{ij}^{R}\,Y_{ij}^{R})}{\sum_j \sum_i (Y_{ij}^{Q}\,Y_{ij}^{Q} + Y_{ij}^{R}\,Y_{ij}^{R})}. \tag{2}$$

For a given set of source parameters the scalar factor C is calculated according to equation (2). This C value is subsequently inserted into equation (1) to given an estimate of the error count S. The scalar factor C yields an estimate of the seismic moment of the earthquake.

In order to find a set of source parameters whose theoretical spectra will yield a minimum error count S, each of the four source parameters is varied systematically

by increments in a prescribed range. The error counts associated with any two successive sets of source parameters are compared and the smaller one is retained for comparison with the next set of source parameters. At the end a minimum error count S is found and the corresponding set of source parameters is taken as the best solution of the source mechanism and focal depth for the earthquake.

For the purpose of finding source mechanisms and focal depths of earthquakes in the Eurasian continent by the program just described, a continental model consisting of a 40-km crust will be used. For a given set of observed surface wave spectra, the following range and increment of the four source parameters are prescribed for finding the best-fit theoretical spectra.

	Range	Increment
Strike (ϕ)	$0 \sim 180°$	10°
Dip angle (δ)	$20 \sim 90°$	10°
Slip angle (λ)	$-90° \sim 90°$	30°
Focal depth (h)	$0 \sim 70$ km	5 km

The method has been applied to a limited number of earthquakes for which the present results can be checked against other independent evidence. The results are described below.

Fig. 12 shows the observed and the best-fit theoretical spectra of Rayleigh and Love waves for Event B2 which is an earthquake located on the Anatolian fault in

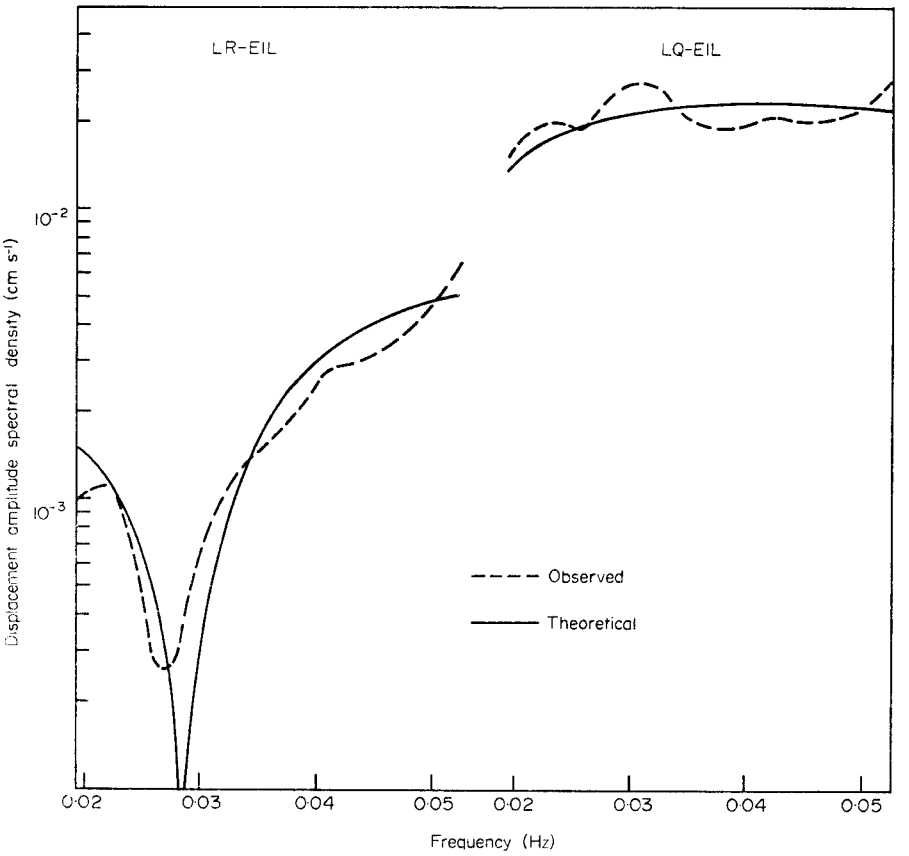

FIG. 12. Observed and theoretical displacement amplitude spectral density of Rayleigh (LR) and Love (LQ) waves for Event B2.

Eastern Turkey. The dashed and solid curves represent the observed and theoretical spectra, respectively. The observed spectra shown in the figure have been corrected for instrument response and geometrical spreading. The agreement between the observed and theoretical spectra is good not only in individual spectral shapes but also in the relative spectral levels of the two types of waves. The source parameters associated with these theoretical spectra are the following: $h = 35$ km, $\phi = \text{N } 90° \text{ E}$, $\delta = 90°$, $\lambda = 0°$. Thus, according to the last three parameters, the earthquake was associated with a vertical strike-slip fault running in the E–W direction. This result agrees totally with the Anatolian fault running through the epicentral area. It is interesting to note that the deep node in the observed Rayleigh wave spectrum which was unaltered by the complex cepstrum technique is now closely reproduced in the theoretical spectrum as shown in Fig. 12. This suggests that the complex cepstrum technique is somehow able to distinguish the spectral nodes caused by the multipath interference from those related to the source mechanism and focal depth, and accordingly, will remove only the first type of spectral nodes without affecting the second type of spectral nodes.

Fig. 13 shows the observed and the best-fit theoretical spectra of Love and Rayleigh waves for Event B3 which is an earthquake in Eastern Turkey. Again the dashed and solid curves represent the observed and theoretical spectra, respectively. The source parameters associated with the theoretical spectra give a focal depth of 15 km and a fault-plane solution defined by the following two nodal planes: (I) $\phi = \text{N } 10° \text{ E}$, $\delta = 80°$, $\lambda = 0°$; (II) $\phi = \text{N } 100° \text{ E}$, $\delta = 90°$, $\lambda = -10°$. This fault plane solution agrees very well with a solution obtained from the polarities of P wave first motions obtained by Canitez & Toksöz (1971) for an earthquake taking place on 1967 July 26, in the same epicentral area as Event B3. They also determined that the focal depth of the same earthquake was 12 km using surface wave spectral data at a number of recording sites. Our value of 15 km for the focal depth of Event B3 is again in excellent agreement with their result.

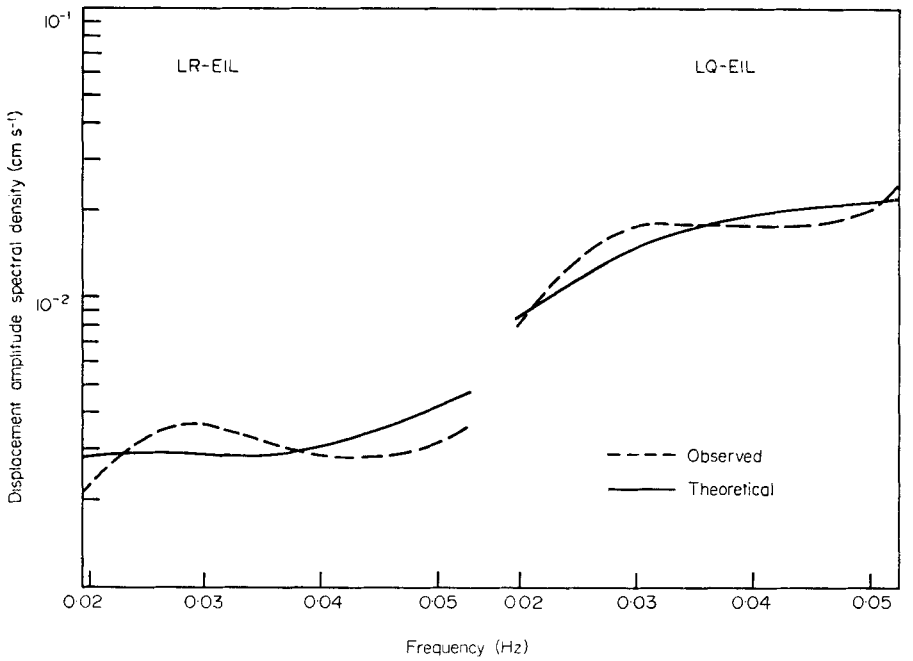

FIG. 13. Observed and theoretical displacement amplitude spectral density of Rayleigh (LR) and Love (LQ) waves for Event B3.

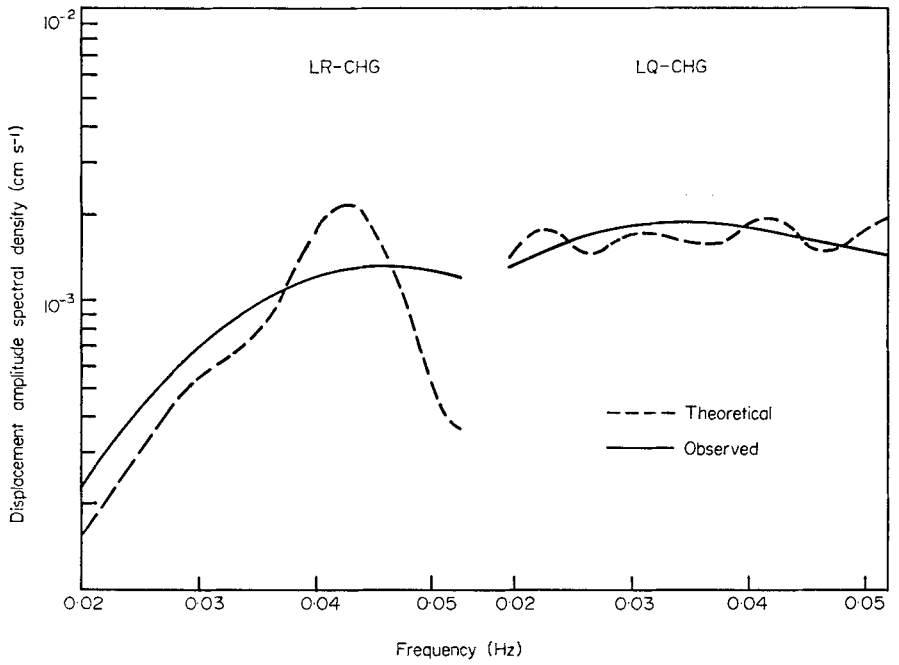

FIG. 14. Observed and theoretical displacement amplitude spectral density of Rayleigh (LR) and Love (LQ) waves for Event E2.

Fig. 14 shows the observed and the best-fit theoretical spectra of Love and Rayleigh waves from Event E2 which is an earthquake in Tadzhik–Sinkiang border region. The dashed and solid curves represent the observed and theoretical spectra, respectively. The agreement between them is again quite good. The source parameters corresponding to the best-fit spectra yield a focal depth of 45 km and a fault plane solution containing one nodal plane defined by the following three parameters: $\phi = \text{N}\,110^\circ\,\text{E}$, $\delta = 60^\circ$, $\lambda = 60^\circ$. This source mechanism agrees very well with the fault plane solutions for several earthquakes located in the same epicentral area as Event E2 reported by Shirokava (1967).

In summary, the positive results from the preceding three examples suggest that reliable estimates of the focal depth and source mechanism of an earthquake can be obtained by the method described above using Love and Rayleigh wave spectra at a small number of recording sites. As shown in Table 1, the m_b magnitudes of Events B2, B3, and E2 are 4·8, 4·7, and 4·8, respectively. For these relatively small earthquakes it is often difficult, if not impossible, to determine their focal depths and source mechanism by conventional methods of using teleseismic body wave data. For these earthquakes the present method, when supplemented with the complex cepstrum technique, offers a practical means for determining their source parameters from a small amount of surface wave spectral data. With the deployment of the high-gain long-period seismographs around the world, the number of earthquakes whose parameters can be determined by this method will be substantial.

Acknowledgment

This research was supported by the Advanced Research Projects Agency, Nuclear Monitoring Research Office, under Project VELA-UNIFORM, and accomplished under the direction of the Air Force Office of Scientific Research under Contract

No. F44620-71-C-0112. Assistance in programming and data analysis by Messrs S. A. Benno and Wen-Wu Shen is appreciated.

Texas Instruments Inc.,
c/o Seismic Array Analysis Center,
314 *Montgomery Street,*
Alexandria, Virginia 22314.

References

Canitez, N. & Toksöz, M. N., 1971. Focal mechanisms and source depth of earthquakes from body- and surface-wave data, *Bull. seism. Soc. Am.*, **61,** 1369–1379.

Linville, A. F., 1971. Rayleigh-wave multipath analysis using a complex cepstrum technique: Special Rpt. No. 2, Long-period array processing development, *Texas Instruments Incorporated, Services Group*, Dallas, Texas.

Saito, M., 1967. Excitation of free oscillations and surface waves by a point source in a vertically heterogeneous earth, *J. geophys. Res.*, **72,** 3689–3699.

Schafer, R. W., 1969. *Echo removal by discrete generalized linear filtering*, Ph.D. Thesis, Technical Rpt 466, Mass. Inst. of Tech., Research Laboratory of Electronics, Cambridge, Massachusetts.

Skirokova, E. I., 1967. General features in the orientation of principal stresses in earthquake foci in the Mediterranean–Asian seismic belt, *Izv. Earth Phys.* (English Translation), **1,** 22–36.

Sykes, L. R., 1967. Mechanism of earthquakes and nature of faulting on the mid-oceanic ridges, *J. geophys. Res.*, **72,** 2131–2153.

Tsai, Y. B. & Aki, K., 1970. Precise focal depth determination from amplitude spectra of surface waves, *J. geophys. Res.*, **75,** 5729–5743.

Tsai, Y. B. & Aki, K., 1971. Amplitude spectra of surface waves from small earthquakes and underground nuclear explosions, *J. geophys. Res.*, **76,** 3940–3952.